

Light curves of jetted gamma-ray burst afterglows in circumstellar clouds

Z. G. Dai, Y. F. Huang, and T. Lu

Department of Astronomy, Nanjing University, Nanjing 210093, China

(accepted for publication in *MNRAS Letters*)

ABSTRACT

The afterglow emission from a spreading jet expanding in a circumstellar cloud is discussed. Prompt X-ray radiation and a strong UV flash from the reverse shock produced by the interaction of the jet with the cloud may destroy and clear the dust out to about 30 pc within the initial solid angle of the jet. As the sideways expansion of the jet becomes significant, most of the optical radiation from the high-latitude part of the jet may be absorbed by the dust outside the initial solid angle of the jet, but only the radiation from the part within the initial solid angle can be observed. We analytically show that the flux of the observational radiation decays as $\propto t^{-(p+1)}$ (where p is the power-law index of the electron distribution) in the relativistic phase. This preliminary result motivates us to perform numerical calculations. Our results show that one break in the optical afterglow light curve extends over a factor of ~ 3 in time rather than one decade in time in the previous jet model. These results may provide a way to judge whether GRBs locate in dense clouds or not. Finally, we carry out a detailed modelling for the R-band afterglow of GRB 000926.

Key words: gamma-rays: bursts — dust: extinction — stars: formation

1 INTRODUCTION

The origin of gamma-ray bursts (GRBs) has puzzled us for more than three decades (see, e.g., Wijers, Rees & Mészáros 1997; Wijers 1998). In the study of GRBs, two fundamental questions pertinent directly to the central engine need to be solved urgently and unambiguously. One question is about the existence of jets in GRBs. Multi-wavelength observations of

afterglows have provided several indications of jetted GRBs: theoretically, it is first shown analytically that the sideways expansion (Rhoads 1999; Sari, Piran & Halpern 1999) and edge effects of jets (Mészáros & Rees 1999) can lead to a marked break in afterglow light curves, and subsequent calculations indicate that one break appears but extends over at least one decade in time (Moderski, Sikora & Bulik 2000; Kumar & Panaiteescu 2000; Huang et al. 2000a, b, c; Wei & Lu 2000). These effects seem to account for the observed light curves of the optical afterglows from GRB 990123 (Kulkarni et al. 1999; Castro-Tirado et al. 1999; Fruchter et al. 1999), GRB 990510 (Harrison et al. 1999; Stanek et al. 1999), GRB 990705 (Masetti et al. 2000a), GRB 991208 (Sagar et al. 2000a; Galama et al. 2000a), GRB 991216 (Halpern et al. 2000a), and GRB 000301C (Rhoads & Fruchter 2001; Masetti et al. 2000b; Jensen et al. 2000; Berger et al. 2000; Sagar et al. 2000b). Further evidence for a jet-like geometry in GRBs is the observed radio flares from GRB 990123 (Kulkarni et al. 1999) and GRB 990510 (Harrison et al. 1999). In addition, the polarization observed in some afterglows also provides an important signature for jetted GRBs (Wijers et al. 1999).

Another question is about the association of GRBs with star-forming regions. There is considerable evidence linking the progenitors of GRBs with massive stars. For example, the sources of the GRBs with known redshifts lie within the optical radii and central regions of the host galaxies rather than far outside the disks of the galaxies (Bloom, Kulkarni & Djorgovski 2000), which seems to rule out mergers of neutron-star binaries as the GRB central engine. Further evidence has been provided by the fact that the brightness distribution of GRBs is in agreement with the models in which the GRB rate tracks the star formation rate over the past 15 billion years of cosmic history (Totani 1997; Wijers et al. 1998; Kommers et al. 2000). The most direct evidence for the relation between GRBs and a specific type of supernova (i.e., hypernovae/collapsars) is the discovery of SN 1998bw in the error box of GRB 980425 (Galama et al. 1998) and the detection of a supernova-like component in the afterglows from GRB 980326 (Bloom et al. 1999) and GRB 970228 (Reichart 1999; Galama et al. 2000b). Finally, the recent discovery of a transient absorption edge in the X-ray spectrum of GRB 990705 (Amati et al. 2000) and the observations of X-ray lines from GRB 991216 (Piro et al. 2000) and GRB 000214 (Antonelli et al. 2000) provide new evidence that GRBs are related to the core collapse of massive stars. Based on these observational facts, it is natural to suppose that the environments of GRBs should be pre-burst winds

and/or circumstellar clouds. If GRBs occur in such pre-burst winds, their afterglows will fade down rapidly (Dai & Lu 1998; Chevalier & Li 1999, 2000); if GRBs are surrounded by the circumstellar clouds, their fireballs (or jets) must evolve to the non-relativistic regime within a few days after the bursts, leading to a steepening of the afterglow light curves (Dai & Lu 1999, 2000; Wang, Dai & Lu 2000).

The purpose of this paper is to combine these two fundamental points to discuss their implications instead of directly proving their existence. We assume that a GRB comes from a highly collimated jet expanding in a circumstellar cloud, and discuss the resultant afterglow emission when the jet is spreading laterally. In section 2, we analyze the motivation of our work: a strong UV flash from the reverse shock produced by the interaction of the jet with the cloud may clear the dust out to about 30 pc only along the initial path of the GRB. As a result, most of the optical radiation from the high-latitude part of the jet may be strongly extinguished by the dust outside the initial solid angle of the jet, but only the radiation from the part within the initial solid angle can be observed. One expects that this could produce a rapidly fading afterglow. In section 3, we further analyze the spectrum and light curve. In section 4, we present our numerical procedure and results. We carry out a detailed modelling for the R-band afterglow of GRB 000926 in section 5, and give a brief discussion and summary in the final section.

2 MOTIVATION

In the standard afterglow model (for recent reviews see Piran [1999] and van Paradijs, Kouveliotou & Wijers [2000]), a GRB relativistic shell with a Lorentz factor of η is assumed to interact with the ambient medium (circumstellar cloud) via two shocks: a reverse shock and a forward shock. The forward shock runs forward into the cloud while the reverse shock sweeps up the shell material. The observed prompt optical flash of GRB 990123 has been argued to come from a reverse shock (Akerlof et al. 1999; Sari & Piran 1999; Mészáros & Rees 1999). We believe that reverse shock emission should be common for all GRBs. The shocked cloud and shell materials are in pressure balance and are separated by a contact discontinuity. Since an optical flash is produced when the reverse shock crosses the shell, the shocked materials expand with a Lorentz factor of γ , which is approximated by the Blandford-MeKee's self-similar solution. As argued by Waxman & Draine (2000), the reverse

shock (with a Lorentz factor of γ^{rs}) may be mildly relativistic, i.e., $|\gamma^{\text{rs}} - 1| \sim 1$, and thus $\gamma \sim \eta$. We assume that the power-law index of the electron distribution, p , is similar in the forward and reverse shocks. If the fractions of the thermal energy carried by electrons, ϵ_e , and magnetic field, ϵ_B , are also similar in the two shocks, then the typical electron Lorentz factor in the reverse shock $\gamma_m^{\text{rs}} \approx 610\xi\epsilon_e$ and the magnetic field $B \approx (32\pi\eta^2nm_pc^2)^{1/2}$, where $\xi = 3(p-2)/(p-1) \approx 1$ and n is the baryon number density of the cloud.

We consider synchrotron radiation from the reverse shock. To calculate the luminosity of the optical flash, one needs to know the emission spectrum, which is determined by two break frequencies: the peak frequency ν_m^{rs} and the cooling frequency ν_c^{rs} . We first derive the observed peak synchrotron frequency:

$$\nu_m^{\text{rs}} \approx 5.8 \times 10^{12} \xi^2 \epsilon_{e,-1}^2 \epsilon_{B,-6}^{1/2} \eta_{300}^2 n_3^{1/2} \left(\frac{1+z}{2} \right)^{-1} \text{Hz}, \quad (1)$$

where $\epsilon_{e,-1} = \epsilon_e/0.1$, $\epsilon_{B,-6} = \epsilon_B/10^{-6}$, $\eta_{300} = \eta/300$, and $n_3 = n/10^3 \text{ cm}^{-3}$. The cooling frequency can be approximately expressed as

$$\nu_c^{\text{rs}} \sim 10^{19} \epsilon_{B,-6}^{-3/2} \epsilon_{54}^{-1/2} n_3^{-1} t_1^{-1/2} \left(\frac{1+z}{2} \right)^{1/2} \text{Hz}, \quad (2)$$

where t_1 is the observer's time (t) in units of 10 s (Wang, Dai & Lu 2001). In addition, using equation (4) of Waxman & Draine (2000), we find the observed peak synchrotron flux density for the reverse shock

$$F_{\nu_m}^{\text{rs}} \approx 40 \epsilon_{B,-6}^{1/2} \eta_{300}^{-1} n_3^{1/4} \epsilon_{54}^{5/4} t_1^{-3/4} \left(\frac{1+z}{2} \right)^{3/4} \left(\frac{\sqrt{1+z} - 1}{\sqrt{2} - 1} \right)^{-2} \text{Jy}, \quad (3)$$

where $\epsilon = \epsilon_{54} \times 10^{54} \text{ ergs sr}^{-1}$ is the shell energy per unit solid angle, z is the redshift of the source, and a flat universe with zero cosmological constant and the Hubble constant $H_0 = 65 \text{ km s}^{-1} \text{ Mpc}$ is assumed. Therefore, we get the spectrum

$$F_{\nu}^{\text{rs}} = \begin{cases} (\nu/\nu_m^{\text{rs}})^{-(p-1)/2} F_{\nu_m}^{\text{rs}} & \text{if } \nu_m^{\text{rs}} < \nu < \nu_c^{\text{rs}}, \\ (\nu_c^{\text{rs}}/\nu_m^{\text{rs}})^{-(p-1)/2} (\nu/\nu_c^{\text{rs}})^{-p/2} F_{\nu_m}^{\text{rs}} & \text{if } \nu > \nu_c^{\text{rs}}. \end{cases} \quad (4)$$

From this spectrum, we can easily calculate the local-frame prompt luminosity ($L_{1-7.5}$) in the 1–7.5 eV range (*UV band*). For example, if $p = 2.5$, we find

$$L_{1-7.5} \sim 1 \times 10^{50} \epsilon_{e,-1}^{3/2} \epsilon_{B,-6}^{7/8} \eta_{300}^{1/2} n_3^{5/8} \epsilon_{54}^{5/4} t_1^{-3/4} \left(\frac{1+z}{2} \right)^{3/4} \text{ergs s}^{-1}. \quad (5)$$

Please note that Waxman & Draine (2000) calculated the UV luminosity at $p = 2$. Here we have extended their discussion to any given p .

We turn to discuss dust destruction in a circumstellar cloud with a typical radius of

$R_c \sim 30$ pc. Since the column density of the cloud is $N_H = nR_c \approx 10^{23}n_3(R_c/30 \text{ pc}) \text{ cm}^{-2}$, the inferred visual extinction is $\sim 50n_3(R_c/30 \text{ pc})$ if the cloud is assumed to have the same dust-to-gas ratio as the Galactic clouds, implying that an afterglow from the GRB would be completely extinguished without dust destruction. Fortunately, as argued by Waxman & Draine (2000), a strong UV flash from the GRB can destroy its ambient dust by thermal sublimation. Using their equation (17), we find that the dust grains are completely sublimed out to a destruction radius $R_d \approx 30(L_{1-7.5}/10^{50} \text{ ergs s}^{-1})^{1/2}$ pc, where the grain radius $a = 0.1 \mu\text{m}$ is assumed. Thus, a strong UV flash with luminosity of $\sim 10^{50} \text{ ergs s}^{-1}$, if isotropic, can clear all the dust grains in a typical giant molecular cloud. Furthermore, Fruchter, Krolik & Rhoads (2001) show that if a GRB emits X-rays in a way similar to those observed by BeppoSAX, dust grains along the line of sight at a distance as large as ~ 100 pc in the host galaxy of the burst can be destroyed by these prompt X-rays due to grain heating and charging. These results were recently confirmed by Galama & Wijers (2001), who analyzed a complete sample of GRB afterglows, and found that the GRB environments have both high column densities ($\sim 10^{23} \text{ cm}^{-2}$) of gas and low optical extinctions. However, since the GRB is believed to come from a jet with the initial half opening angle of $\theta_0 \sim 0.1$, the UV flash and prompt X-ray emission will clear the dust only along the initial path of the burst. Therefore, the optical radiation from the $\theta \leq \theta_0$ part has low extinction but the optical radiation from the high-latitude ($\theta > \theta_0$) part could be absorbed by the dust outside the initial solid angle of the jet, implying that only an afterglow emission from the low-latitude of the jet would be observed if the line of sight is along the jet axis. This could lead to a rapidly fading optical afterglow. Motivated by this argument, we will discuss the afterglow emission from a spreading jet expanding in a circumstellar cloud in the next section.

3 ANALYTICAL MODEL: SPECTRUM AND LIGHT CURVE

Rhoads (1999) has considered the evolution of a *relativistic* jet (with Lorentz factor of γ) that is spreading laterally at the local speed of sound $c_s = c/\sqrt{3}$ (but $c_s = c$ in Sari et al. [1999]), so the half opening angle $\theta_j \sim \theta_0 + \gamma^{-1}/\sqrt{3}$. In this case, the dynamical transition takes place at $\gamma \sim \theta_0^{-1}/\sqrt{3}$. In the initial stage of the evolution, since $\gamma > \theta_0^{-1}/\sqrt{3}$, the jet is spherical-like and its Lorentz factor decays as $\gamma \propto t^{-3/8}$. The resulting spectrum and light curve are well known (Sari, Piran & Narayan 1998):

$$F_\nu^{\text{fs}} \propto \begin{cases} \nu^{-(p-1)/2} t^{-3(p-1)/4} & \text{if } \nu_m^{\text{fs}} < \nu < \nu_c^{\text{fs}}, \\ \nu^{-p/2} t^{-(3p-2)/4} & \text{if } \nu > \nu_c^{\text{fs}}. \end{cases} \quad (6)$$

We next stress to discuss the afterglow emission for $\gamma \ll \theta_0^{-1}/\sqrt{3}$. In this spreading stage, the sideways expansion leads to an exponential decay of γ with radius (Rhoads 1999; Sari et al. 1999). As a result, the jet's radius $R \propto t^0$ and $\gamma \propto t^{-1/2}$. The typical synchrotron frequency decays as $\nu_m^{\text{fs}} \propto t^{-2}$ and the cooling frequency ν_c^{fs} is a constant. From the discussion in section 2, the total number of electrons radiating toward to the observer, those located in a cone of the initial opening angle, can be estimated as $N_e = \pi\theta_0^2 R^3 n/3$. The total specific luminosity emitted by these electrons, $(1+z)\sigma_T m_e c^2 N_e B' \gamma / (3e)$, is distributed over an area of $\pi\gamma^{-2} D_L^2$ at the luminosity distance D_L from the source (where B' is the magnetic field strength of the shocked cloud). Thus, the observed peak flux density is given by $F_{\nu_m}^{\text{fs}} = (1+z)\sigma_T m_e c^2 R^3 n \theta_0^2 B' \gamma^3 / (9e D_L^2) \propto R^3 \gamma^4 \propto t^{-2}$. Therefore, we obtain the afterglow's spectrum and light curve:

$$F_\nu^{\text{fs}} = \begin{cases} (\nu/\nu_m^{\text{fs}})^{1/3} F_{\nu_m}^{\text{fs}} \propto \nu^{1/3} t^{-4/3} & \text{if } \nu < \nu_m^{\text{fs}}, \\ (\nu/\nu_m^{\text{fs}})^{-(p-1)/2} F_{\nu_m}^{\text{fs}} \propto \nu^{-(p-1)/2} t^{-(p+1)} & \text{if } \nu_m^{\text{fs}} < \nu < \nu_c^{\text{fs}}, \\ (\nu_c^{\text{fs}}/\nu_m^{\text{fs}})^{-(p-1)/2} (\nu/\nu_c^{\text{fs}})^{-p/2} F_{\nu_m}^{\text{fs}} \propto \nu^{-p/2} t^{-(p+1)} & \text{if } \nu > \nu_c^{\text{fs}}. \end{cases} \quad (7)$$

It is easy to see that the temporal decay index of the high-frequency afterglow changes from $\alpha_1 = 3(p-1)/4$ or $(3p-2)/4$ to $\alpha_2 = p+1$ because of the effects of sideways expansion and dust extinction. In conclusion, a marked break should appear in the light curve of the afterglow from a spreading jet expanding in the circumstellar giant cloud.

4 NUMERICAL RESULTS

To prove the analytical result in section 3, we perform detailed numerical calculations for the evolution of the afterglow emission. We use the model proposed by Huang, Dai & Lu (1999) and the calculational code developed by Huang et al. (2000c). This model has several advantages: (i) It is applicable to both radiative and adiabatic jets, and proper for both ultra-relativistic and non-relativistic stages. The model even allows the radiative efficiency ϵ to change with time, so that it can trace the evolution of a partially radiative jet (Dai, Huang & Lu 1999). However, note that some authors (e.g., Mészáros, Rees & Wijers 1998) have argued that the jet should be adiabatic most likely, since it is unlikely that the radiative efficiency

could reach 1; (ii) The model considers the lateral expansion of the jet. The evolution of the lateral speed (taken as the speed of sound) is given by a reasonable expression (see equation [12]). (iii) The model also takes into account many other effects, e.g., *the cooling of electrons and the equal arrival time surfaces*. Let M_{ej} be the initial ejecta mass and m the swept-up cloud mass. The dynamical evolution of the jet is described by (Huang et al. 2000c)

$$\frac{dR}{dt} = \beta c\gamma(\gamma + \sqrt{\gamma^2 - 1}), \quad (8)$$

$$\frac{d\theta_j}{dt} = \frac{c_s(\gamma + \sqrt{\gamma^2 - 1})}{R}, \quad (9)$$

$$\frac{dm}{dR} = 2\pi R^2(1 - \cos\theta_j)nm_{\text{p}}, \quad (10)$$

$$\frac{d\gamma}{dm} = -\frac{\gamma^2 - 1}{M_{\text{ej}} + \epsilon m + 2(1 - \epsilon)\gamma m}, \quad (11)$$

$$c_s^2 = \frac{\hat{\gamma}(\hat{\gamma} - 1)(\gamma - 1)c^2}{1 + \hat{\gamma}(\gamma - 1)}, \quad (12)$$

where $\beta = \sqrt{1 - 1/\gamma^2}$ and $\hat{\gamma} \approx (4\gamma + 1)/(3\gamma)$ (Dai et al. 1999). If $\epsilon \rightarrow 0$ as in the following calculations, equation (11) turns out to express the conservation of energy: $(\gamma - 1)M_{\text{ej}} + (\gamma^2 - 1)m = \text{constant}$ (for a discussion see Huang et al. [1999] and van Paradijs et al. [2000]).

Figure 1 presents light curves of R-band afterglow emission ($p = 2.5$) for two cases with dust extinction (*solid line*) and without dust extinction (*dashed line*). This figure clearly shows that the light curve with dust extinction is indeed more steepening than that without dust extinction at late times. Figure 2 exhibits $\alpha \equiv -d\ln F_R/d\ln t$ as a function of time for these two cases. For the case without dust extinction, α increases from ~ 1.3 at initial one day to ~ 2.5 at later times. This change extends over one order of magnitude in time, which is consistent with the previous numerical results (Moderski et al. 2000; Kumar & Panaiteescu 2000; Huang et al. 2000a, b, c). However, for the case with dust extinction, α increases from ~ 1.3 at initial one day to ~ 3.3 at later times, which is in approximate accord with the analytical result in section 3. Furthermore, the steepening is completed over a factor of ~ 3 in time, leading therefore to a sharper break in the light curve.

5 AFTERGLOW OF GRB 000926

GRB 000926 was detected on 2000 September 26.9927 UT by the Inter-Planetary-Network (IPN) group of spacecrafts Ulysses, Russian Gamma-Ray Burst Experiment (KONUS) and

Near Earth Asteroid Rendezvous (NEAR) (Hurley et al. 2000). The burst lasted ~ 25 s and had a $25 - 100$ keV fluence of $\sim 2.2 \times 10^{-5}$ ergs cm $^{-2}$. The redshift of the source was determined at $z = 2.0369 \pm 0.0007$ (Castro et al. 2000), yielding a luminosity distance of $D_L = 16.9$ Gpc. The optical light curve of the afterglow from GRB 000926 fell off as $\sim t^{-1.1 \pm 0.2}$ for the first $t_{\text{br}} = 2.0 \pm 0.4$ days (break time) and subsequently steepened to $\sim t^{-3.2 \pm 0.4}$ (Rol, Vreeswijk & Tanvir 2000). Furthermore, the resultant sharp break extended over a factor of ~ 3 in time, inferred from the fitted function of Rol et al. (2000). In addition, from the optical to X-ray observations, Sagar et al. (2000c) have found that the spectral index $\bar{\beta} = -0.82 \pm 0.02$ at $t = 2.26$. Recently, Price et al. (2001) also fitted a late-time light curve for this afterglow, which slightly flattens as compared with Rol et al.'s (2000).

In our spreading jet model (with dust extinction), the spectral index $\bar{\beta} = -0.82 \pm 0.02$ requires $p = 2.6 \pm 0.08$, implying $\alpha_1 = 1.2 \pm 0.06$ (in the slow cooling regime) prior to the break time t_{br} and subsequently $\alpha_2 = 3.6 \pm 0.08$ (from equation [7]). These values are in excellent agreement with the observations. Figure 3 shows the observed R-band data for GRB 000926 and the theoretically calculated light curve based on the model described in section 4. It can be seen from this figure that our model provides a good fit to the optical afterglow data. More importantly, our model accounts successfully for the observed sharpness of the break that appears in the R-band light curve. We note that the previous spreading jet model (without dust extinction) seems inconsistent with the observed data. This is both because in the previous jet model the temporal decay index increases from ~ 1.3 to ~ 2.6 if $p = 2.6$ and because the sharpness of the observed break cannot be produced in that model, as shown in the present paper and in other studies (e.g., Moderski et al. 2000; Kumar & Panaiteescu 2000; Huang et al. 2000a, b, c).

6 DISCUSSION AND CONCLUSIONS

We have discussed the afterglow emission when a highly collimated jet is spreading laterally and expanding radially in a circumstellar cloud, and have analytically found that the flux decay of the observational optical afterglow changes from $\propto t^{-3(p-1)/4}$ (or $t^{-(3p-2)/4}$) in the relativistic spherical-like phase to $\propto t^{-(p+1)}$ in the relativistic sideways-expansion phase because of strong dust extinction outside the initial solid angle of the jet. This provides a natural explanation for very rapidly fading afterglows. We have also performed numerical

calculations based on the generic afterglow model proposed by Huang et al. (1999) and developed by Huang et al. (2000c). Our numerical results show that one break in the light curve of the optical afterglow extends over a factor of ~ 3 in time in our present model rather than one decade in time in the previous jet model. These results may provide a signature for GRBs in dense clouds. In addition, we have given a good fit to the observed R-band data of the afterglow from GRB 000926.

It is interesting to discuss two effects of dust on afterglows. First, thermal reradiation and scattering outside the destruction radius in the circumstellar giant cloud are expected to cause delayed IR emission (Waxman & Draine 2000; Esin & Blandford 2000), which has been proposed to account for the late-time afterglow feature of GRB 980326 and GRB 970228 instead of the supernova-like component explanation. At $z = 2$ (e.g., GRB 000926), the time delay and the flux for the emission at $2.2 \mu\text{m}$ can be estimated by $t_{\text{IR}} \sim 1.5 \times 10^7 (\theta_0/0.1)^2 (L_{1-7.5}/10^{50} \text{ergs s}^{-1})^{1/2} \text{ s}$, and $F_{2.2 \mu\text{m}} \sim 0.2 (L_{1-7.5}/10^{50} \text{ergs s}^{-1})^{1/2} \mu\text{Jy}$, respectively. This IR flux is expected to be detected in about six months after the burst. Second, since the visual extinction is ~ 50 , the X-rays could be both scattered by the dust grains (e.g., Mészáros & Gruzinov [2000]), whose scattering optical depth at the X-ray energy ϵ_γ is $\tau \approx 15(\epsilon_\gamma/1 \text{ keV})^{-2}$, and efficiently heat the grains. Also, the soft X-rays could be absorbed in the giant dense cloud because of a high optical depth for photo-ionization. These effects may lead to the rapidly fading X-ray afterglow of GRB 000926.

ACKNOWLEDGMENTS

We wish to thank the referee, Dr. Ralph Wijers, for valuable comments, and X. Y. Wang for useful discussions. This work was supported partially by the National Natural Science Foundation of China (grants 19825109, 10003001 and 19773007), by the National 973 Project (NKBRSP G19990754), and by the Special Funds for Major State Basic Research Projects.

REFERENCES

- Akerlof, C. W. et al. 1999, *Nature*, 398, 400
- Amati, L. et al. 2000, *Science*, 290, 953
- Antonelli, L. A. et al. 2000, *ApJ*, 545, L39
- Berger, E. et al. 2000, *ApJ*, 545, 56
- Bloom, J. S. et al. 1999, *Nature*, 401, 453

Bloom, J. S., Kulkarni, S. R., & Djorgovski, S. G. 2000, AJ, submitted (astro-ph/0010176)

Castro, S. M. et al. 2000, GCN Circ. 851

Castro-Tirado, A. J. et al. 1999, Science, 283, 2069

Chevalier, R. A., & Li, Z. Y. 1999, ApJ, 520, L29

Chevalier, R. A., & Li, Z. Y. 2000, ApJ, 536, 195

Dai, Z. G., Huang, Y. F., & Lu, T. 1999, ApJ, 520, 634

Dai, Z. G., & Lu, T. 1998, MNRAS, 298, 87

Dai, Z. G., & Lu, T. 1999, ApJ, 519, L155

Dai, Z. G., & Lu, T. 2000, ApJ, 537, 803

Dall, T. et al. 2000, GCN Circ. 804

Esin, A. A., & Blandford, R. D. 2000, ApJ, 534, L151

Fruchter, A. S. et al. 1999, ApJ, 519, L13.

Fruchter, A. S., Krolik, J. H., & Rhoads, J. E. 2001, ApJ, submitted

Fynbo, J. P. U. et al. 2000a, GCN Circ. 820

Fynbo, J. P. U. et al. 2000b, GCN Circ. 825

Fynbo, J. P. U. et al. 2000c, GCN Circ. 840

Galama, T. J. et al. 1998, Nature, 398, 394

Galama, T. J. et al. 2000a, ApJ, 541, L45

Galama, T. J. et al. 2000b, ApJ, 536, 185

Galama, T. J., & Wijers, R. A. M. J. 2001, ApJ, 549, L209

Gorosabel, J., Castro Ceron, J.M., Castro-Tirado, A.J., & Greiner, J. 2000, GCN Circ. 803

Halpern, J. P. et al. 2000a, ApJ, 543, 697

Halpern, J. P. et al. 2000b, GCN Circ. 824

Halpern, J. P. et al. 2000c, GCN Circ. 829

Harrison, F. A. et al. 1999, ApJ, 523, L121

Hjorth, J. et al. 2000a, GCN Circ. 809

Hjorth, J. et al. 2000b, GCN Circ. 814

Huang, Y. F., Dai, Z. G., & Lu, T. 1999, MNRAS, 309, 513

Huang, Y. F., Dai, Z. G., & Lu, T. 2000a, MNRAS, 316, 943

Huang, Y. F., Dai, Z. G., & Lu, T. 2000b, A&A, 355, L43

Huang, Y. F., Gou, L. J., Dai, Z. G., & Lu, T. 2000c, ApJ, 543, 90

Jensen, B. L. et al. 2001, A&A, in press (astro-ph/0005609)

Kommers, J. M. et al. 2000, ApJ, 533, 696

Kulkarni, S. R. et al. 1999, Nature, 398, 389

Kumar, P., & Panaiteescu, A. 2000, ApJ, 541, L9

Masetti, N. et al. 2000a, A&A, 354, 473

Masetti, N. et al. 2000b, A&A, 359, L23

Mészáros, P., & Gruzinov, A. 2000, ApJ, 543, L35

Mészáros, P., & Rees, M. J. 1999, MNRAS, 306, L39

Mészáros, P., Rees, M. J., & Wijers, R. A. M. J. 1998, ApJ, 499, 301

Moderski, R., Sikora, M., & Bulik, T. 2000, ApJ, 529, 151

Piran, T. 1999, Phys. Rep., 314, 575

Piro, L. et al. 2000, Science, 290, 955

Price, P. A. et al. 2000, GCN Circ. 811

Price, P. A. et al. 2001, ApJL, in press

Reichart, D. E. 1999, ApJ, 521, L111

Rhoads, J. 1999, ApJ, 525, 737

Rhoads, J., & Fruchter, A. S. 2001, ApJ, 546, 117

Rol, E., Vreeswijk, P. M., & Tanvir, N. 2000, GCN Circ. 850

Sagar, R. et al. 2000a, BASI, 28, 15

Sagar, R. et al. 2000b, BASI, 28, 499

Sagar, R. et al. 2000c, astro-ph/0010212

Sari, R., & Piran, T. 1999, ApJ, 517, L109

Sari, R., Piran, T., & Halpern, J. P. 1999, ApJ, 519, L17

Sari, R., Piran, T., & Narayan, R. 1998, ApJ, 497, L17

Stanek, K. Z. et al. 1999, ApJ, 522, L39

Totani, T. 1997, ApJ, 486, L71

van Paradijs, J., Kouveliotou, C., & Wijers, R. A. M. J. 2000, ARA&A, 38, 379

Veillet, C. 2000, GCN Circ. 831

Vrba, F. et al. 2000, GCN Circ. 819

Wang, X. Y., Dai, Z. G., & Lu, T. 2000, MNRAS, 317, 170

Wang, X. Y., Dai, Z. G., & Lu, T. 2001, ApJ, 546, L33

Waxman, E., & Draine, B. T. 2000, ApJ, 537, 796

Wei, D. M., & Lu, T. 2000, ApJ, 541, 203

Wijers, R. A. M. J. 1998, Nature, 393, 13

Wijers, R. A. M. J., Bloom, J. S., Blagla, J. S., & Natarajan, P. 1998, MNRAS, 294, L13

Wijers, R. A. M. J., Rees, M. J., & Mészáros, P. 1997, MNRAS, 288, L51

Wijers, R. A. M. J. et al. 1999, ApJ, 523, L33

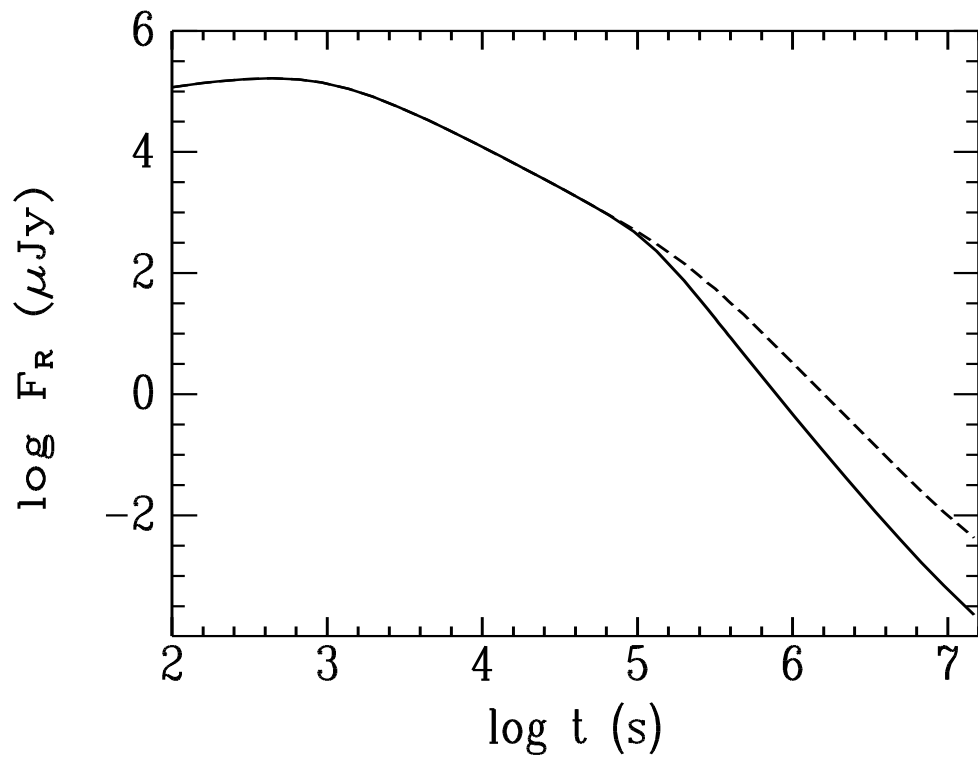


Figure 1. R-band light curves for dust extinction (*solid line*) and no dust extinction (*dashed line*). The model parameters are chosen: $\varepsilon = 10^{54}$ ergs sr^{-1} , $\eta = 300$, $\theta_0 = 0.15$ rad, $p = 2.5$, $n = 10^3$ cm^{-3} , $\epsilon_e = 0.1$, $\epsilon_B = 10^{-6}$, and $D_L = 10$ Gpc.

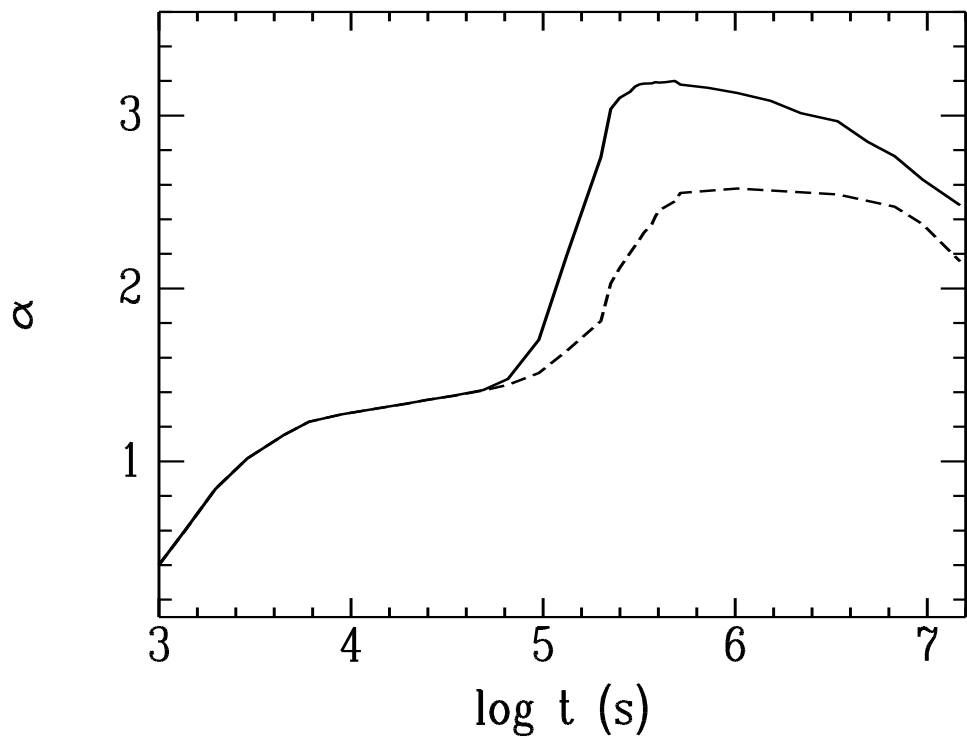


Figure 2. The R-band $\alpha = -d \ln F_\nu / d \ln t$ as a function of time in the cases with dust extinction (solid line) and without dust extinction (dashed line) for the same parameters as in Figure 1.

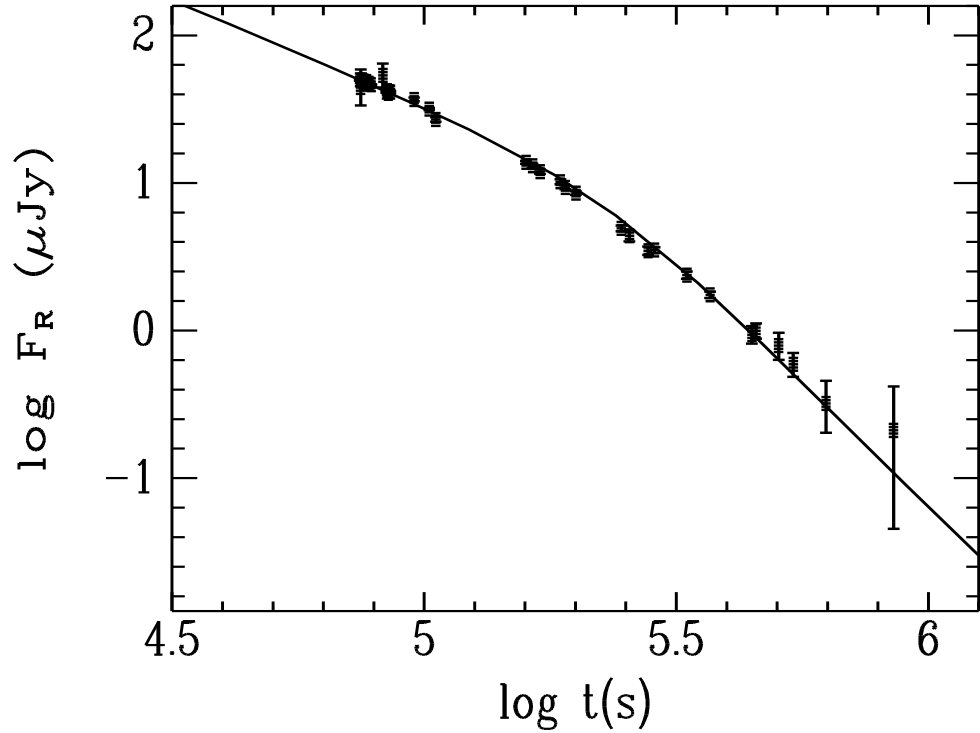


Figure 3. Comparison between the observed and theoretically calculated light curves for the R-band afterglow of GRB 000926. The observational data are taken from GCN Circulars (Gorosabel et al. 2000; Dall et al. 2000; Hjorth et al. 2000a, b; Price et al. 2000; Vrba et al. 2000; Fynbo et al. 2000a, b, c; Halpern et al. 2000b, c; Veillet 2000; Rol et al. 2000), and the model light curve is calculated for a spreading jet expanding in a circumstellar cloud when an observer is located on the jet axis. The model parameters are taken: $\varepsilon = 8 \times 10^{53}$ ergs sr^{-1} , $\eta = 300$, $\theta_0 = 0.2$ rad, $p = 2.6$, $n = 10^3$ cm $^{-3}$, $\epsilon_e = 0.075$, $\epsilon_B = 10^{-7}$, and $D_L = 16.9$ Gpc.